Early Miocene Cyclostratigraphy and Sea-Level Changes from the Pearl River Mouth Basin, South China Sea*

Shi-Feng Tian[1]

Search and Discovery Article #50463 (2011)
Posted August 31, 2011

*Adapted from oral presentation at AAPG Annual Convention and Exhibition, Houston, Texas, USA, April 10-13, 2011

[1]China University of Petroleum, Dongying, China; The University of Western Australia, Perth, WA, Australia (tianshf@yahoo.com.cn)

Abstract

The Pearl River Mouth Basin is situated at offshore shelf of northern part of South China Sea. Recent hydrocarbon exploration indicates that the basin is extremely rich in hydrocarbon resources. However, stratigraphic correlation of the subsurface successions has long been disputed due to absence of their counterparts at outcrop exposures. To improve the stratigraphic resolution for hydrocarbon prospecting and exploration in the basin, this study attempts to undertake detailed cyclostratigraphical analysis of the lower Miocene succession, including:

1) to determine the dominant frequencies of high-frequency cycles based on gamma-ray well-logging data,
2) to test whether Milankovitch orbital signals are registered in the rhythmic succession,
3) to estimate the duration and the net accumulation rate of sequences,
4) to identify and characterize the depositional responses to global and local sea-level changes in a mixed carbonate and siliciclastic setting.

A spectral analysis will be carried out in these wells using the Fourier transform algorithm approach.

Our study indicates that three spatial periods exist in the lower Miocene successions. They vary vertically in the boreholes, but cycle ratios are stable and similar to orbital cycle ratios (i.e., Milankovitch cycles). These three periods correspond to eccentricity, obliquity, and precession, respectively. Since the duration of these orbital cycles are known, depth intervals in the studied wells were converted into time intervals (duration) to establish high-resolution astrochronologic time scales which agree with established biostratigraphic chronology and the International Stratigraphic Chart. The net accumulation rate was generated after calculating the decompaction thickness with regional experienced algorithm. The Miocene sea-level change curves were reconstructed based on integration of biostratigraphic study of relative abundance of planktonic foraminifera and ratio of planktonic/benthic foraminifera, sedimentary facies, astrochronologic, and sequence stratigraphic analyses. At third-order sequence scale, the relative sea-level change curves during the early Miocene in the studied area appear to be similar trends to the global eustatic curves (Haq et al., 1987); both have five 3rd-order rise-fall cycles. However, at higher-order cycle scale, the direction and amplitudes of rise/fall change curves are different from their global equivalents. This disparity may be due to local or regional tectonism.

References

Gradstein, F.M., J.G. Ogg, and A.G. Smith, 2005, A Geologic Time Scale 2004: Cambridge University Press, 610 p.

Haq, B.U., J. Hardenbol, and P.R. Vail, 1987, Chronology of Fluctuating Sea Levels Since the Triassic: Science, v. 235/4793, p. 1156-1167.

Haq, B.U., 1988, Fluctuating Mesozoic and Cenozoic Sea Levels and Implications for Stratigraphy: AAPG Bulletin, v. 72/12, p. 1521.

Laskar, J., P. Robutel, F. Joutel, M. Gastineau, .A.C.M. Correia, and B. Levrard, 2004, Astronomy & Astrophysics, v. 428/1, p. 261-285.

Schwarzacher, W., 2000, Repetitions and Cycles in Stratigraphy: Earth Science Reviews, v. 50/1-2, p. 51-75.

Strasser, M., J. Halfar, and L. Godinez-Orta, 2006, Oceanography, Sedimentology, and Acoustic Mapping of Bryomol Carbonate Factory in the Northern Gulf of California, Mexico *in* Cool-Water Carbonates: Depositional Systems and Palaeoenvironmental Controls: Geological Society of London Special Publication, v. 255, p. 197-215.

Early Miocene Cyclostratigraphy and Sea-level changes from the Pearl River Mouth Basin, South China Sea

Shifeng Tian
PhD Candidate

China University of Petroleum
The University of Western Australia

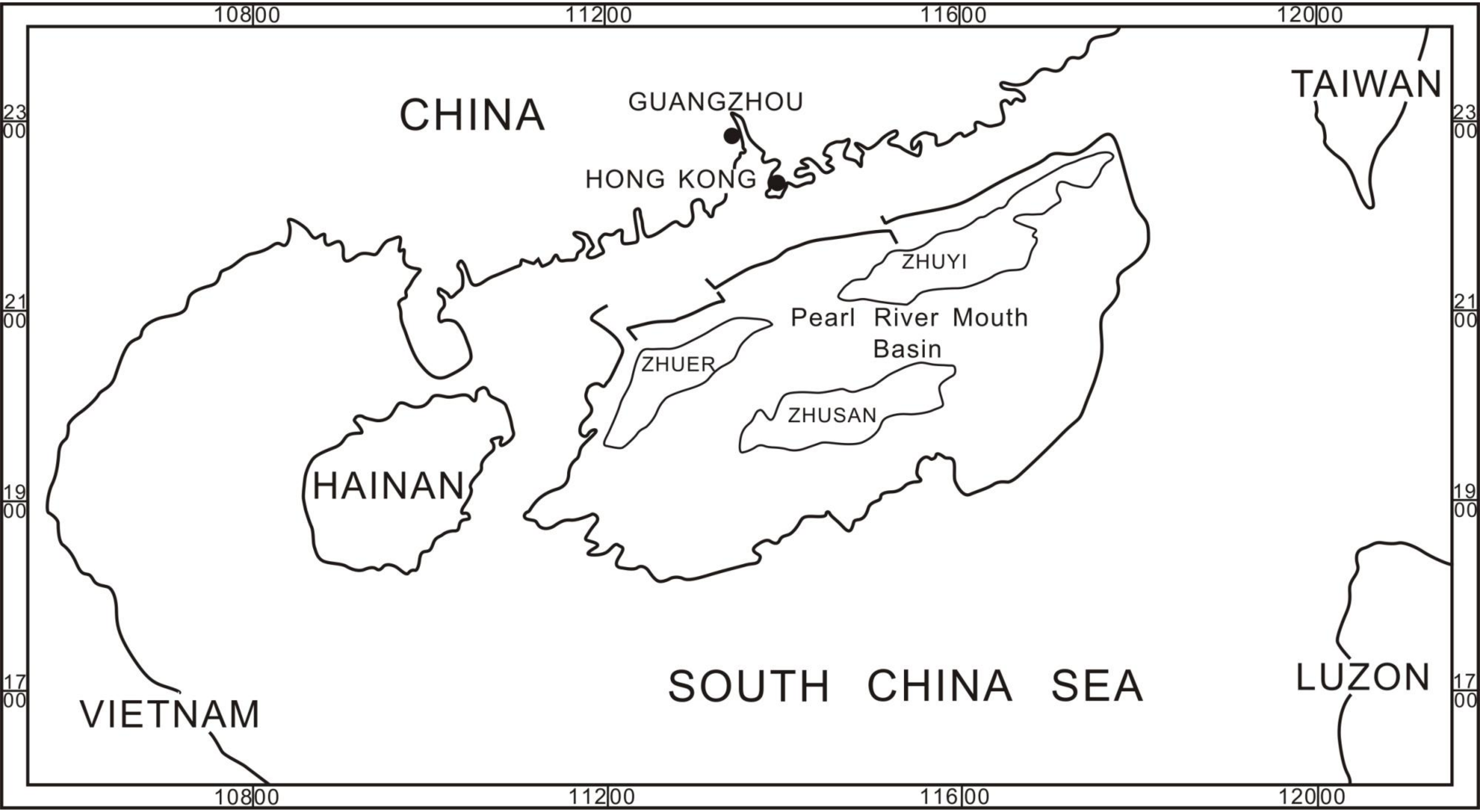

Location of the Pearl River Mouth Basin

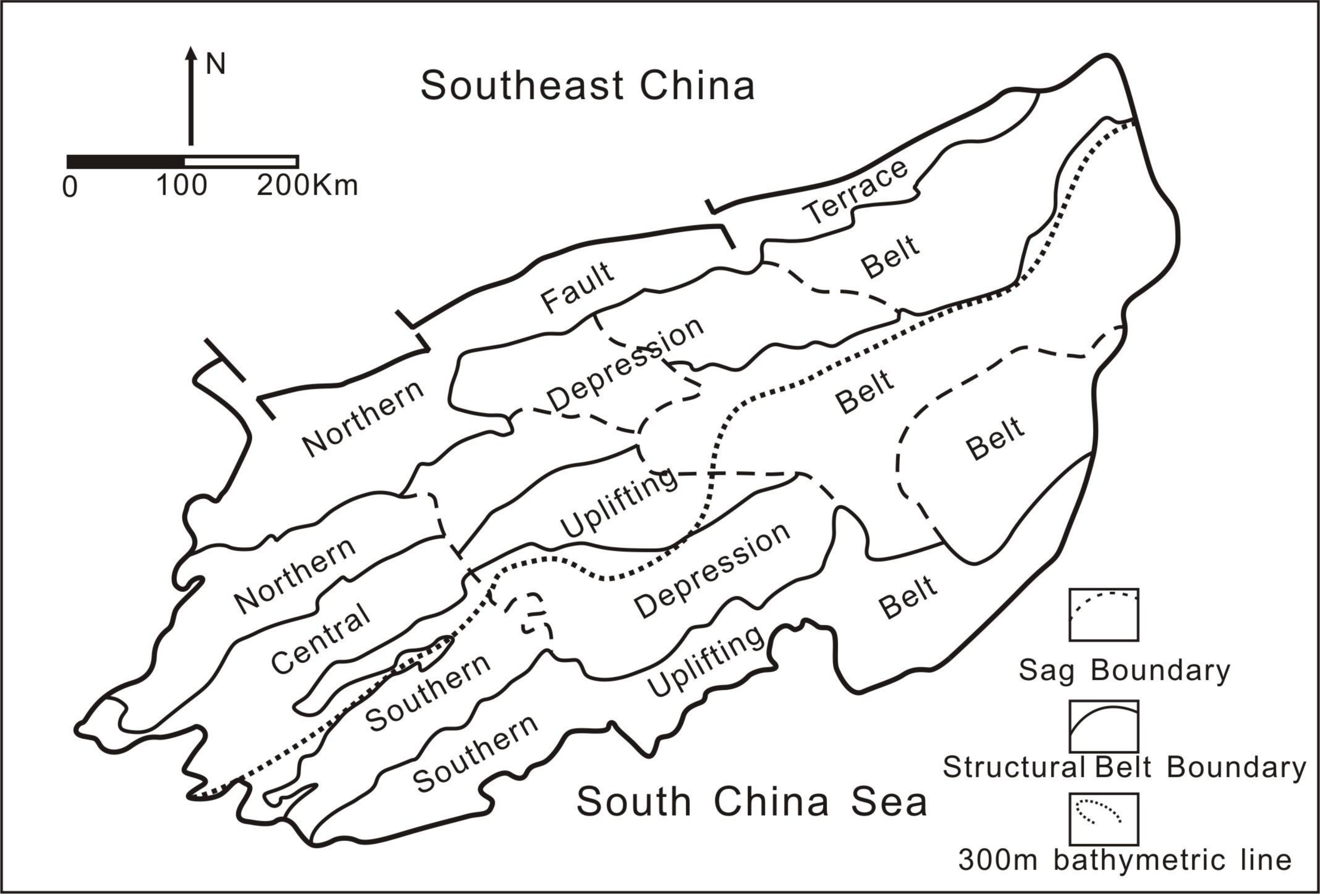

Map showing the structural sub-units of the PRMB

Tectonic movement	From	To
Rifting	Late Cretaceous	Early Oligocene
Depression	Late Oligocene	Early Miocene
Block faulting	Late Miocene	Present

Structural evolution of the Pearl River Mouth Basin

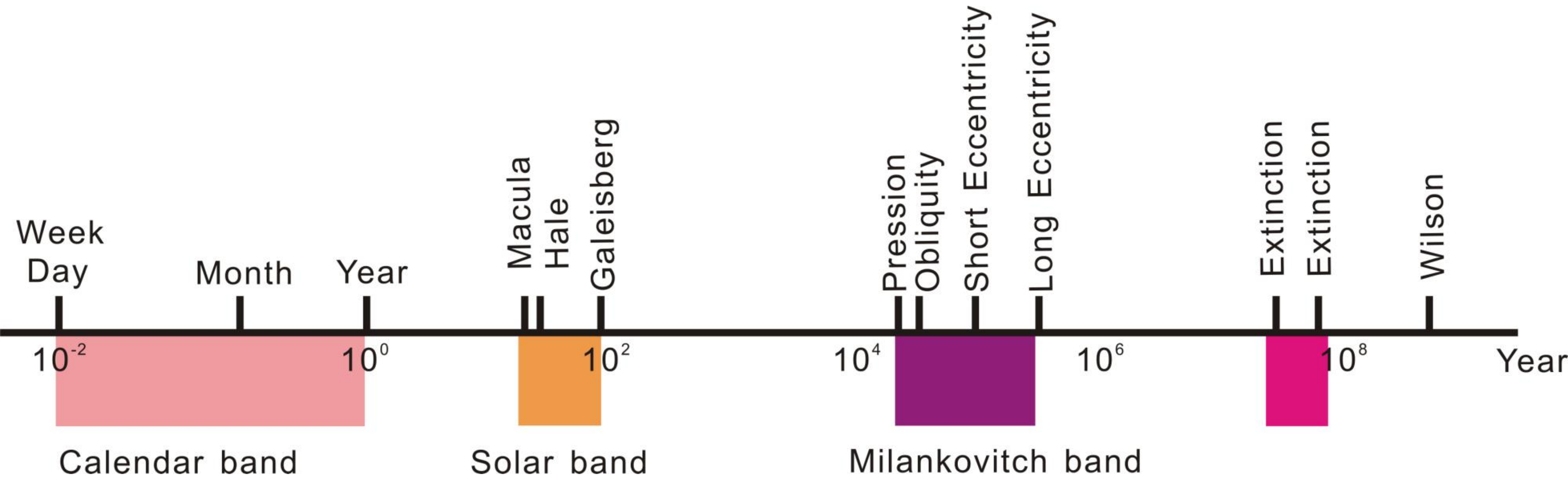

Week
Day
Month
Year
Macula
Hale
Galeisberg
Pression
Obliquity
Short Eccentricity
Long Eccentricity
Extinction
Extinction
Wilson
10^{-2}
10^{0}
10^{2}
10^{4}
10^{6}
10^{8}
Year
Calendar band
Solar band
Milankovitch band

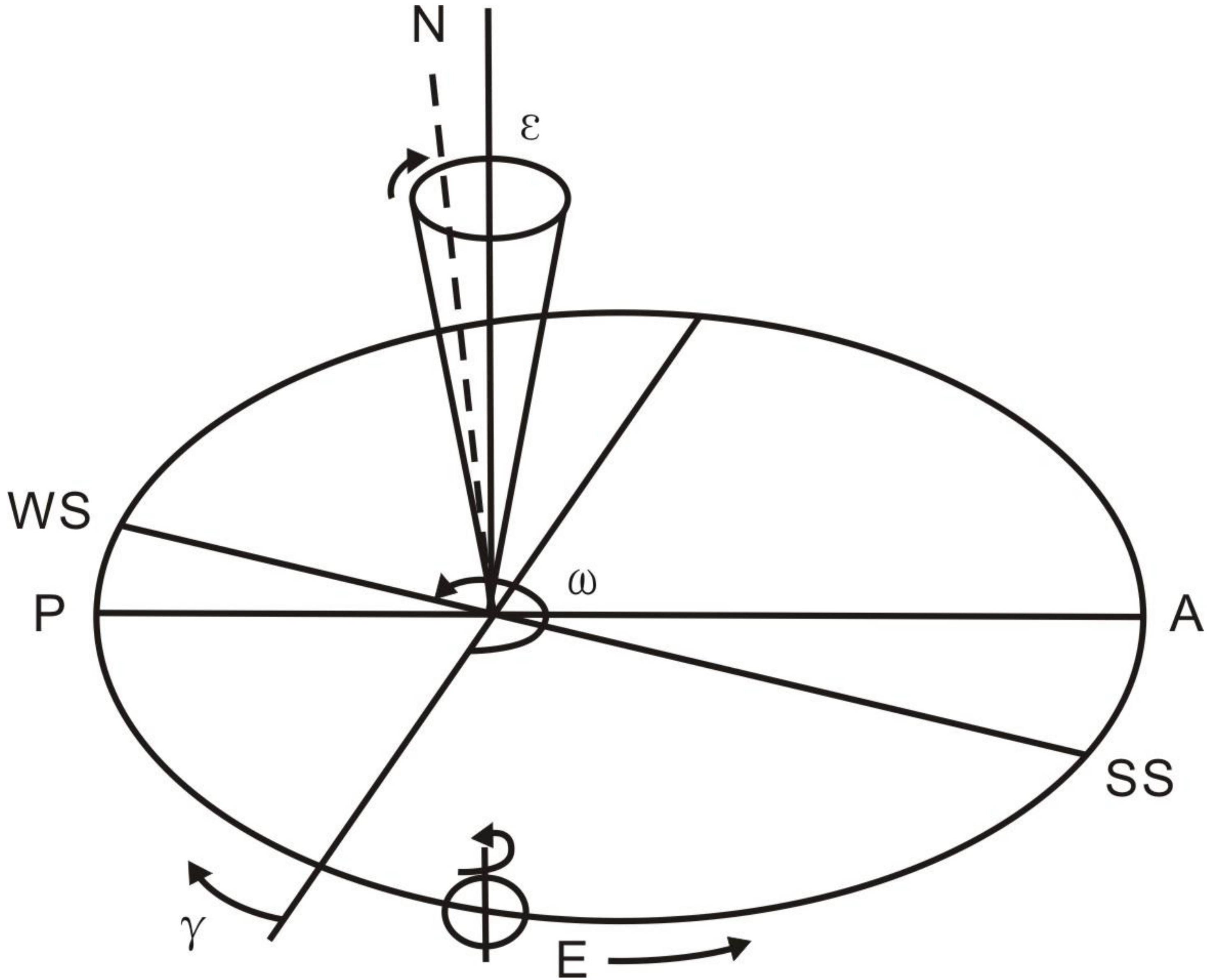

The sun-earth system (according to Schwarzacher, 2000)

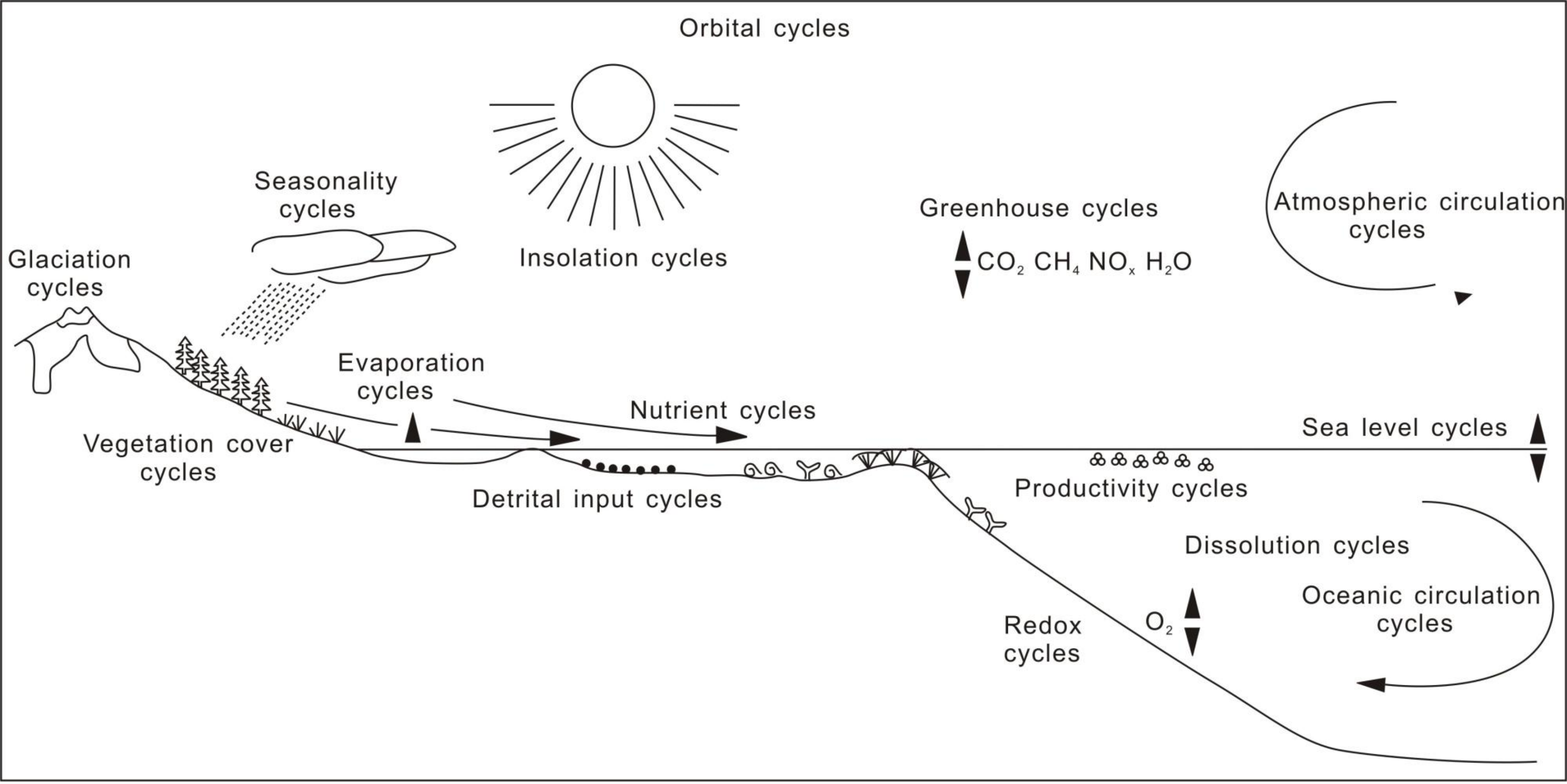

(According to Strasser et al., 2006)

Sketch illustrating the complexity of the atmospheric,oceanic, sedimentary,and biological system that is influenced by orbitally induced insolation changes.

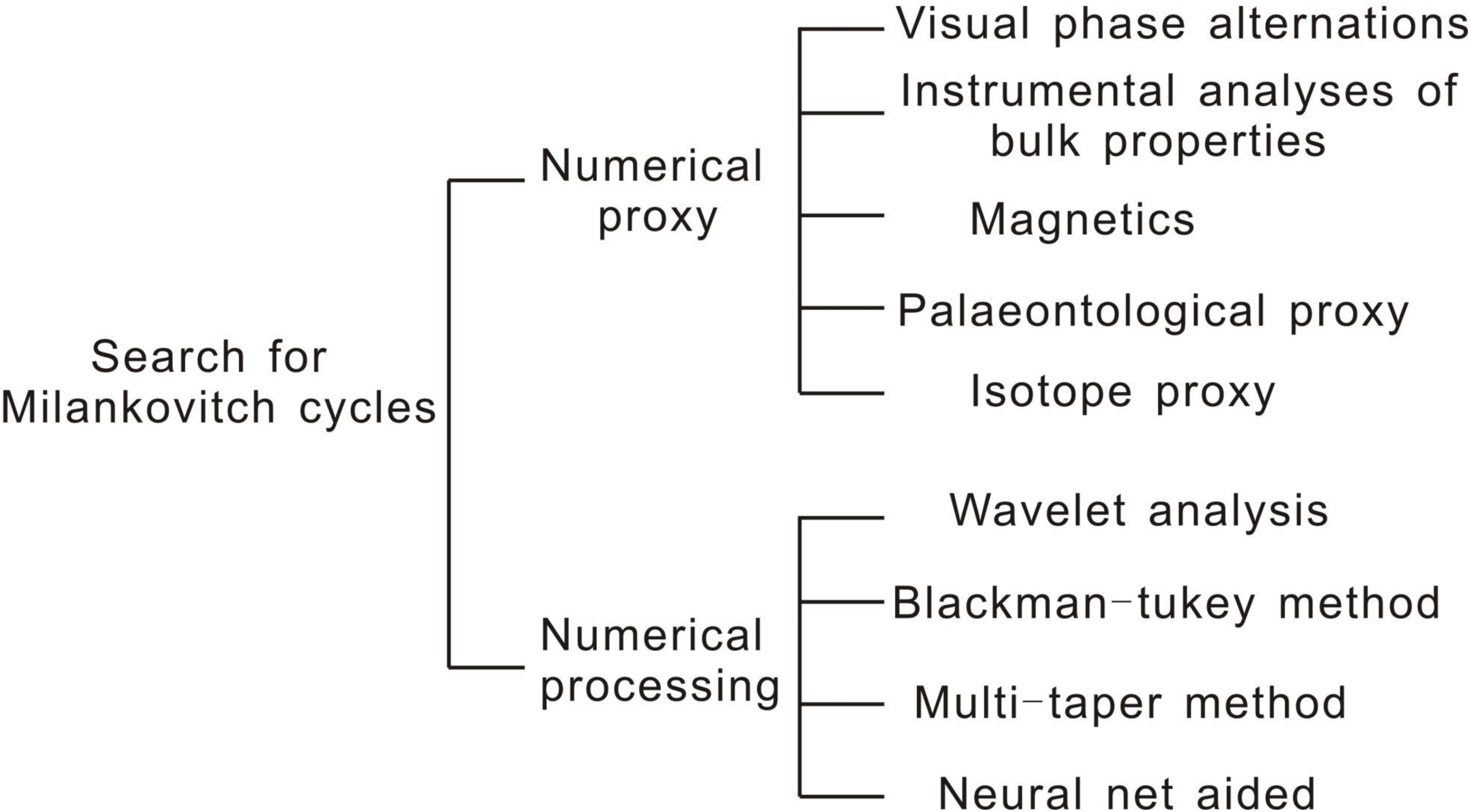
Search for
Milankovitch cycles
Numerical
proxy
Visual phase alternations
Instrumental analyses of
bulk properties
Magnetics
Palaeontological proxy
Isotope proxy
Numerical
processing
Wavelet analysis
Blackman-tukey method
Multi-taper method
Neural net aided

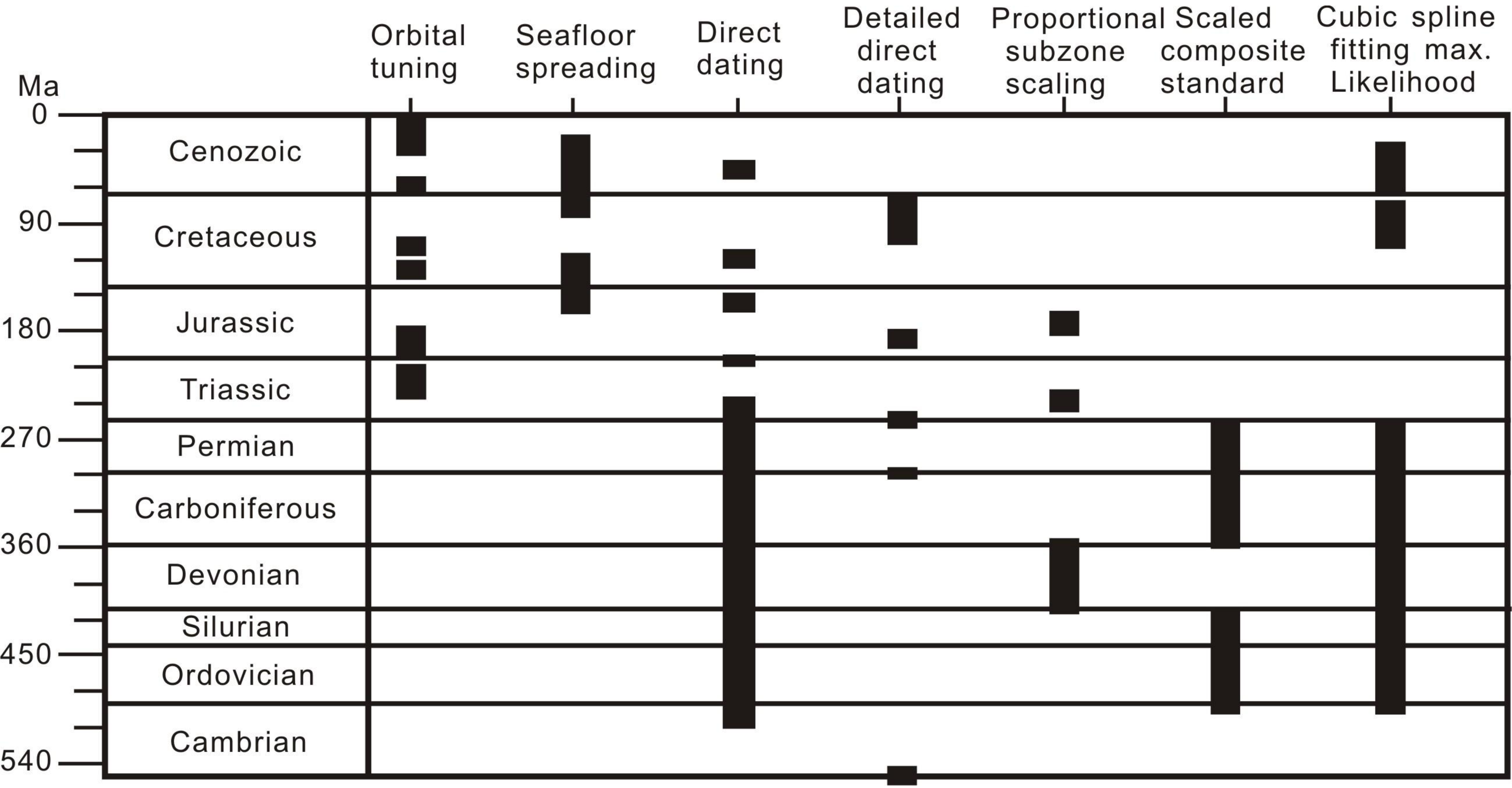

Methods used to construct a Geologic Time Scale 2004 (GTS, 2004)

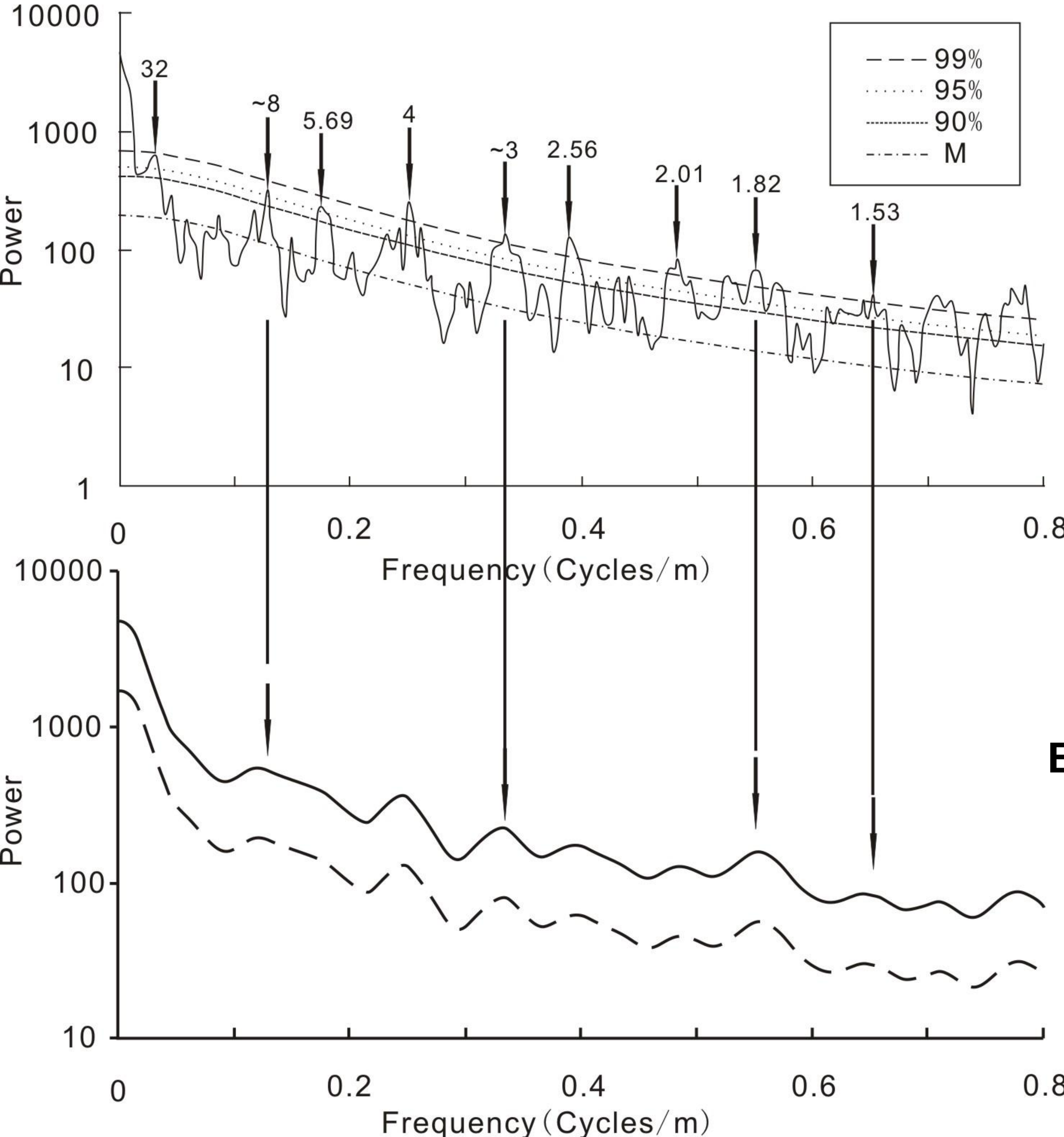

Multi-taper method

Blackman-tukey method

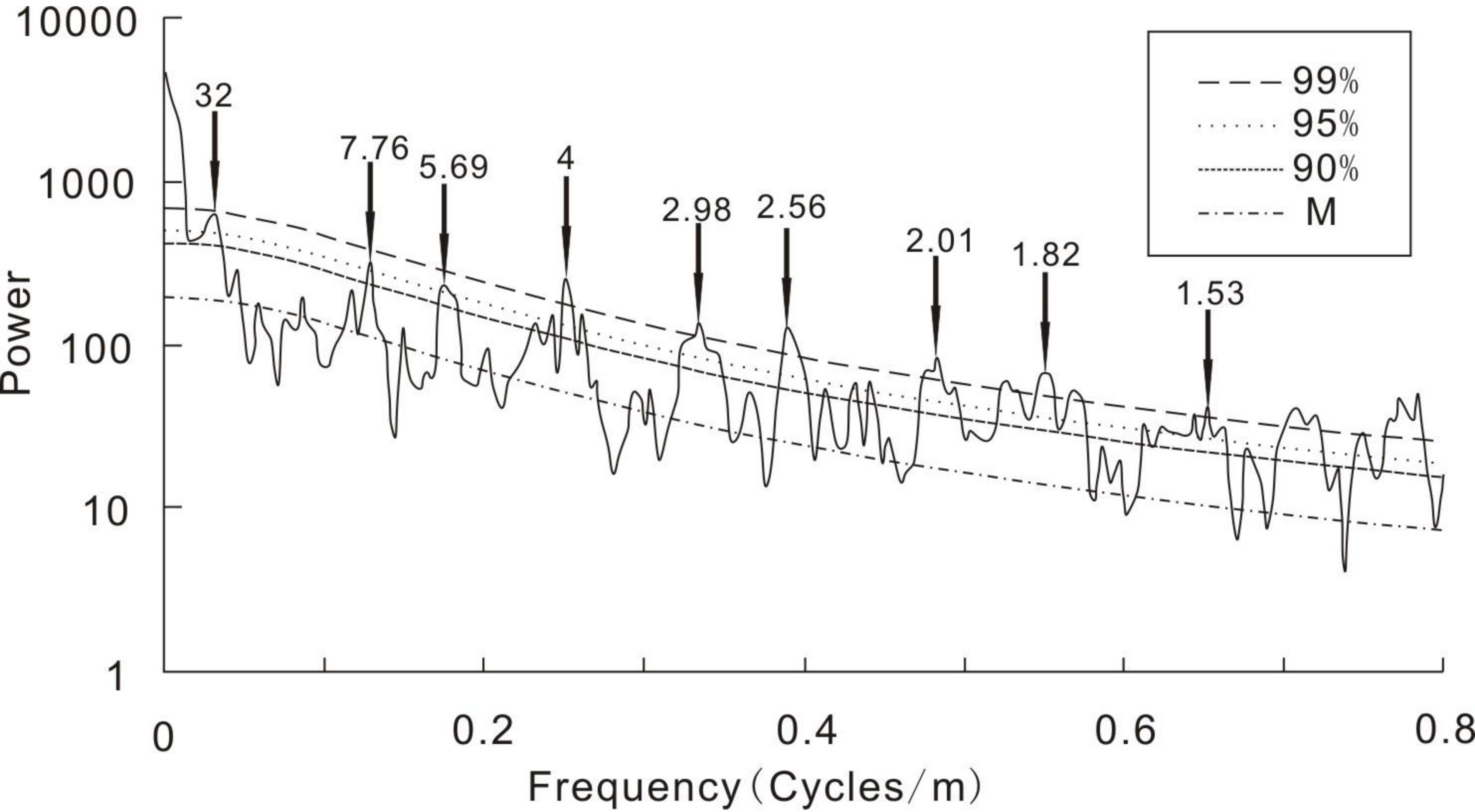

Multi-taper Method

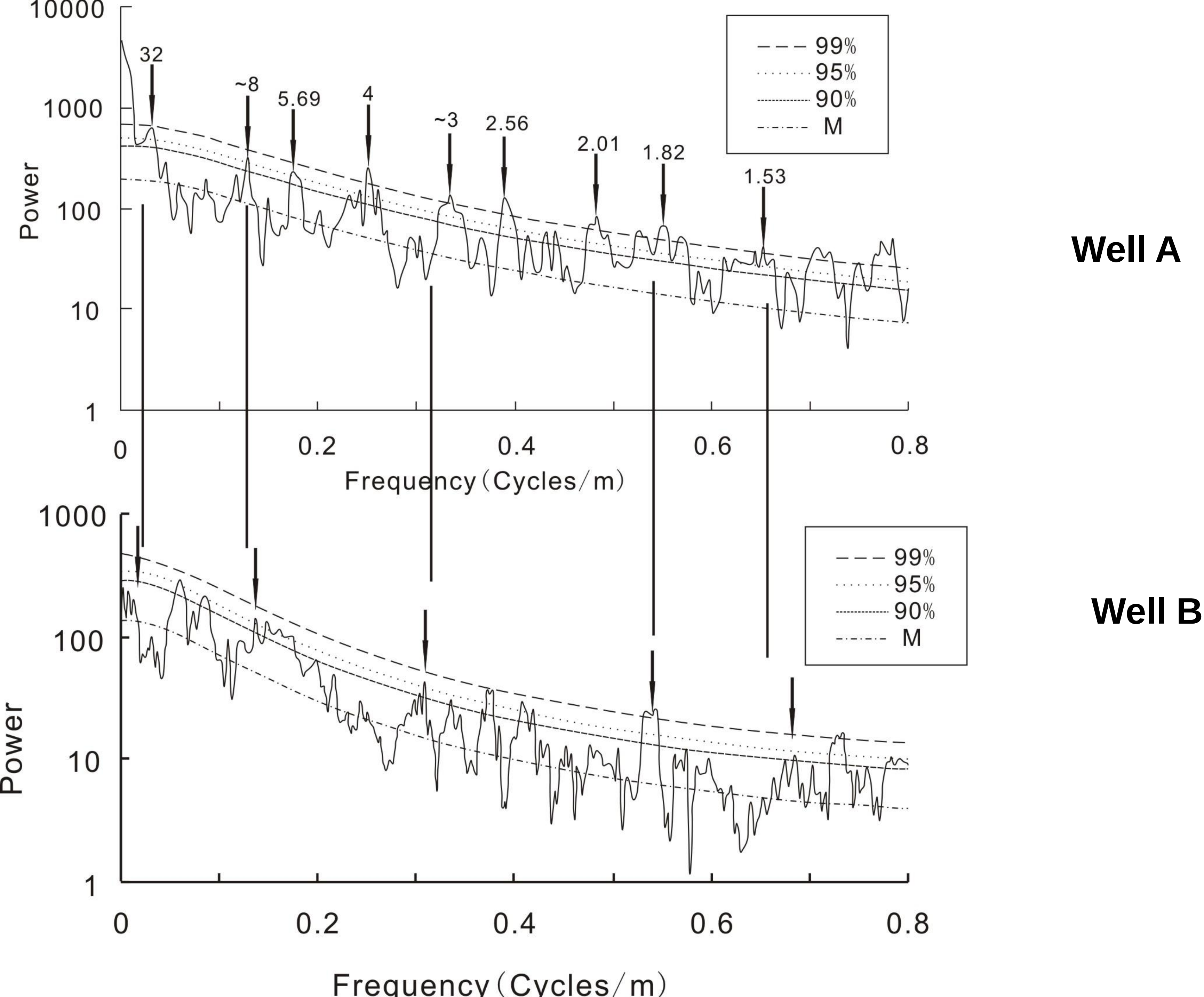

Well A
Power
Frequency（Cycles/m）
32
~8
5.69
4
~3
2.56
2.01
1.82
1.53
99%
95%
90%
M
Well B
Power
Frequency（Cycles/m）
99%
95%
90%
M

GR	Climate	Orbital parameter
Maxima	Warm and wet climate with high organic productivity, enhanced chemical weathering and continental runoff	Maxima insolation Minima obliquity
Minima	Colder and drier	Minima insolation Maxima obliquity

Phase relationships

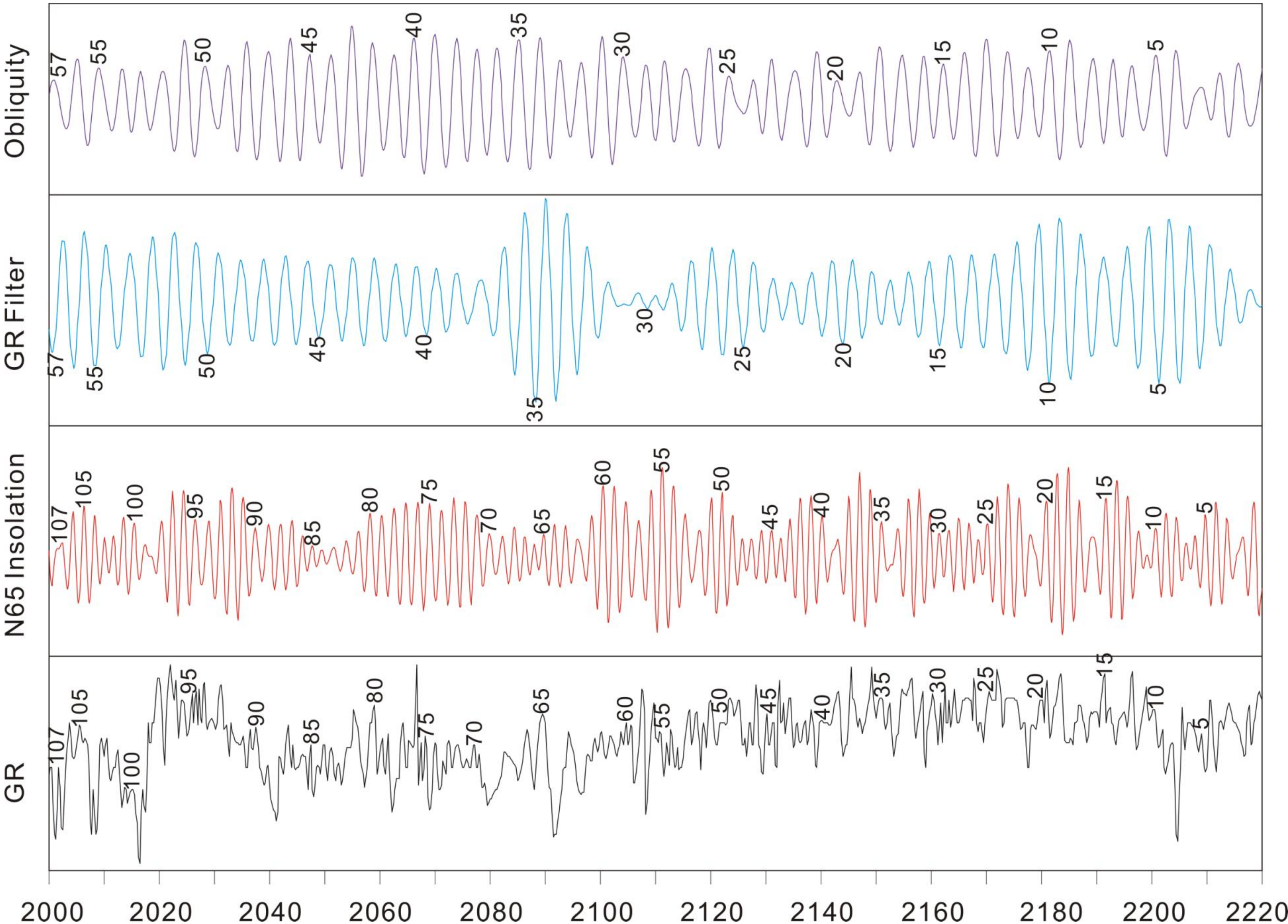

Obliquity
GR Filter
N65 Insolation
GR
2000
2020
2040
2060
2080
2100
2120
2140
2160
2180
2200
2220

Result of astronomical tuning

Depth(m)	Time(Ma)	Depth(m)	Time(Ma)
2000	13.65	2012.25	13.774
2001.25	13.659	2013.25	13.79
2001.75	13.676	2013.5	13.794
2003.75	13.697	2015.25	13.814
2004.5	13.704	2016.5	13.825
2006.5	13.718	2017	13.834
2008	13.738	2020	13.866
2008.5	13.745	2021	13.867
2010.25	13.757	2022	13.887

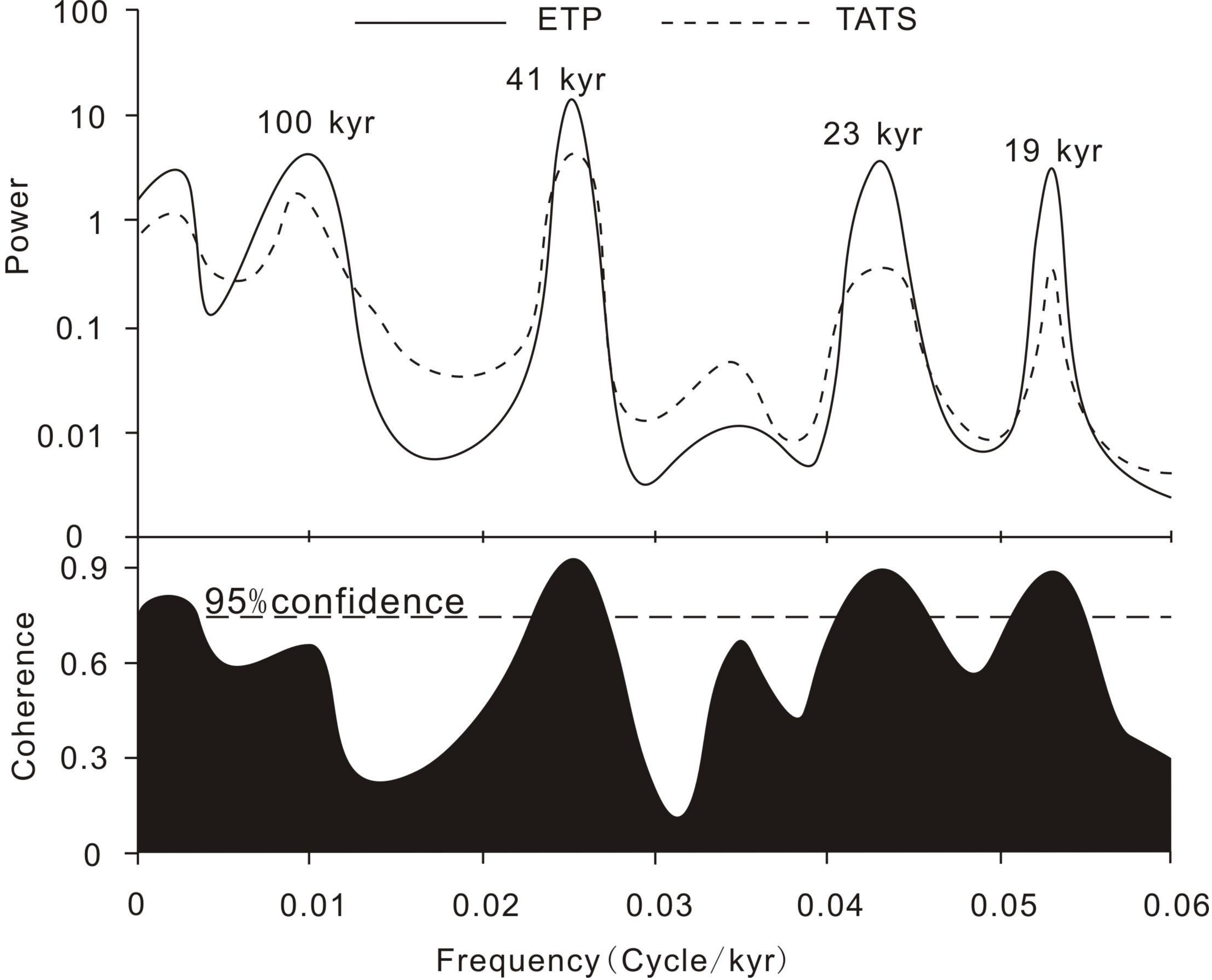

Cross-spectral analysis of the tuned astronomical timescale and ETP

Bioevents (FDO)	Astronomially Estimated Age (Ma)	Thompson (2003)	Error (Ma)
G.peripheroronda	14.919	14.8	0.119
G.sicanus	14.546	14.6	−0.054

FDO=First Downhole Occurrence

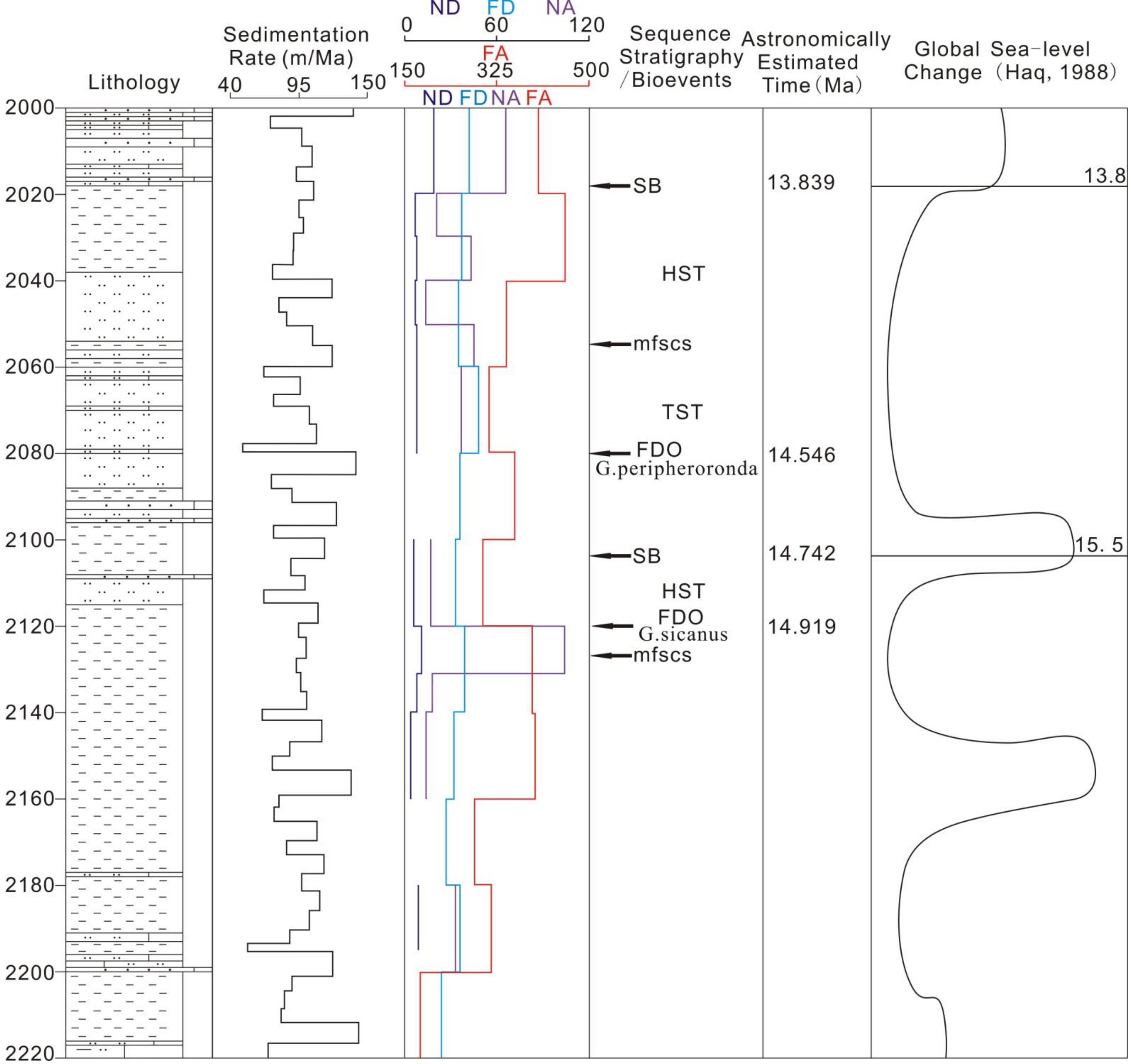

Lithology
Sedimentation Rate (m/Ma)
40 95 150
ND FD NA
0 60 120
FA
150 325 500
ND FD NA FA
Sequence Stratigraphy /Bioevents
Astronomically Estimated Time (Ma)
Global Sea-level Change (Haq, 1988)
2000
2020
2040
2060
2080
2100
2120
2140
2160
2180
2200
2220
SB
HST
mfscs
TST
FDO G.peripheroronda
SB
HST
FDO G.sicanus
mfscs
13.839
14.546
14.742
14.919
13.8
15. 5

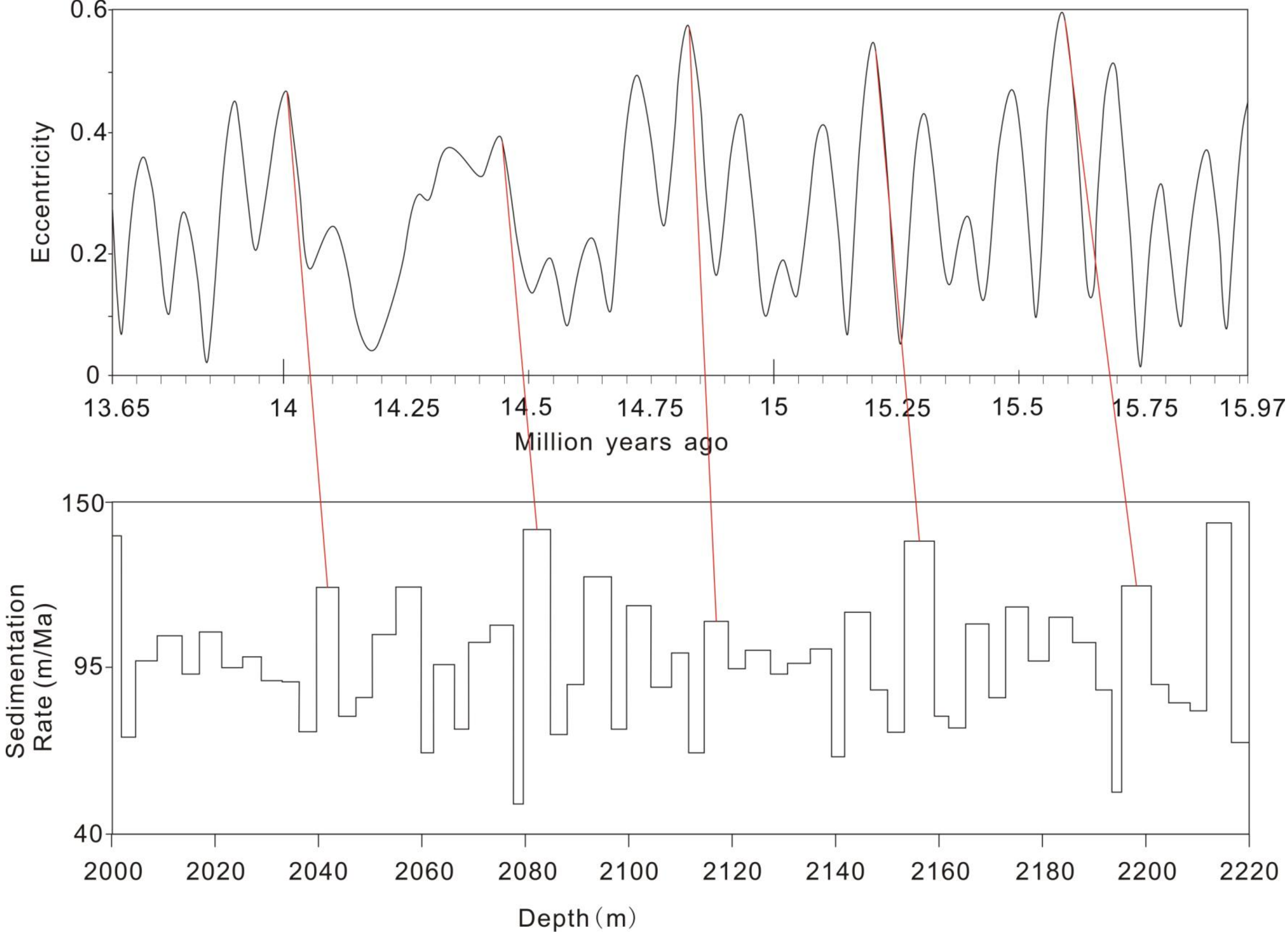

The sedimentation rate compared with Laskar et al., 2004 orbital eccentricity predicted over 13.65- 15.97 Ma

Thank you!!!

tianshf@yahoo.com.cn